THE AMERICAN SOCIETY OF MECHANICAL ENGINEERS
345 E. 47 St., New York, N.Y. 10017

90-GT-95

Prediction and Measurement of Film Cooling Effectiveness for a First-Stage Turbine Vane Shroud

D. GRANSER and T. SCHULENBERG
Siemens AG
Postfach 10 17 55
D-4330 Mülheim
Fed. Rep. Germany

Abstract

After compressor discharge air has initially been used to cool the heat shields of the hot gas inlet casing, it can subsequently be employed for film cooling of the first-stage vane shrouds. Since the flow field near these shrouds is three-dimensional, the film cooling effectiveness cannot be predicted correctly by common two-dimensional codes. The secondary flow transports the film from the pressure side to the suction side where it can even climb up the airfoil to cool its trailing section.

Such film cooling effectiveness was first investigated experimentally in a linear vane cascade at atmospheric pressure. The temperatures and static pressure levels at the adiabatic shrouds, as well as the temperature measurements within the vane cascade, are reported for different cooling film blowing rates.

In addition, the secondary flow was analysed numerically using a partially-parabolic computer code for 3D viscous flows. It involves mutual interaction of the boundary layer with the mainstream. The secondary flow can also be modelled with this algorithm, which requires less numerical effort than solving the fully 3D elliptic flow equations. The numerical results of the experiment and numerical predictions are compared. In addition, the application of these results to a high-temperature gas turbine is presented.

Introduction

The increased gas temperature and pressure in modern high temperature gas turbines require more and more efficient cooling of turbine shrouds, especially of the first stage turbine vane. These shrouds have not been critical in the past. With high turbine inlet temperatures, however, the cooling air consumption of the shroud approaches that of the airfoil, so that we need to optimize their cooling arrangement.

Sealing air which has been released in front of the stage, as well as remaining cooling air of preceding stages or of the transition piece between combustor and turbine, help to minimize the additional cooling air for these shrouds. Thereby, the gas temperature at the shrouds is colder than that at the airfoil, which provides a quite effective film cooling. Moreover, even the trailing portion of the airfoil's suction side is cooled down additionally, because the cooling film on the shrouds is transported to the suction side by secondary flow. There it generates a cold spot, which has been demonstrated on a first stage blade by Schulenberg and Bals (1986).

We can take advantage of this film cooling especially at the leading portion of the shrouds. Towards the trailing portion, however, the film temperature increases because of mixing with the outer flow, so that additional cooling of the shrouds is required. It was the aim of this study to develop a model to predict this film cooling effectiveness.

*Presented at the Gas Turbine and Aeroengine Congress and Exposition—June 11-14, 1990—Brussels, Belgium

The boundary layer, and therefore also the film cooling effectiveness on the shrouds, is highly effected by secondary flow phenomena. It was already pointed out by Langston (1980) that the conventional 2-D boundary layer approach is expected to fail to predict these phenomena. Years later, Jilek (1986) studied the secondary flow vortices in more detail, but his results suggest that general empirical formulas are too simple to predict secondary flow.

A qualitative impression of the trajectories of this cooling film has been given by Moore and Smith (1984). For prediction of pressure losses they injected ethylene into the boundary layer in front of the horseshoe vortex near the leading edge. Near the stage exit they detected more than 65% of this ethylene concentrated in a vortex which is placed in the corner of the endwall next to the suction side of the airfoil. Gaugler and Russell (1983) also visualized this vortex with soap bubble traces in the boundary layer. Their experiment, too, confirms that the film is not spread uniformly over the shroud.

Some special experiments on film cooling effectiveness of a first stage vane shroud have been performed by Bourguignon (1985). There, deviating from our study, the cooling film has been supplied through rows of impinging jets in the shroud. Quantitative results, however, have not been published.

Recent progresses in modelling the 3D viscous flow in turbine cascades encourage us to expect that endwall boundary layers can be predicted numerically. Some isothermal 3D flow calculations by Dawes (1986) show that secondary flow losses are quite well reproduced by solving the full 3D Navier-Stokes equations. A similar attempt has been made here by applying a partially-parabolic algorithm which is described in more detail below.

In order to validate this code an atmospheric test rig has been installed. Film cooling effectiveness as well as gas temperatures have been measured.

Test Facility

The test rig, Fig. 1, represents a simplification of the real passage around the first guide vane. Size and parameters are listed in Tab. 1. The test rig consisted of a linear vane cascade, preceded by a rectangular duct through which ambient air was sucked in. Duct and vanes were made of plexiglass. The ratio of the duct length to its height was 2.5.

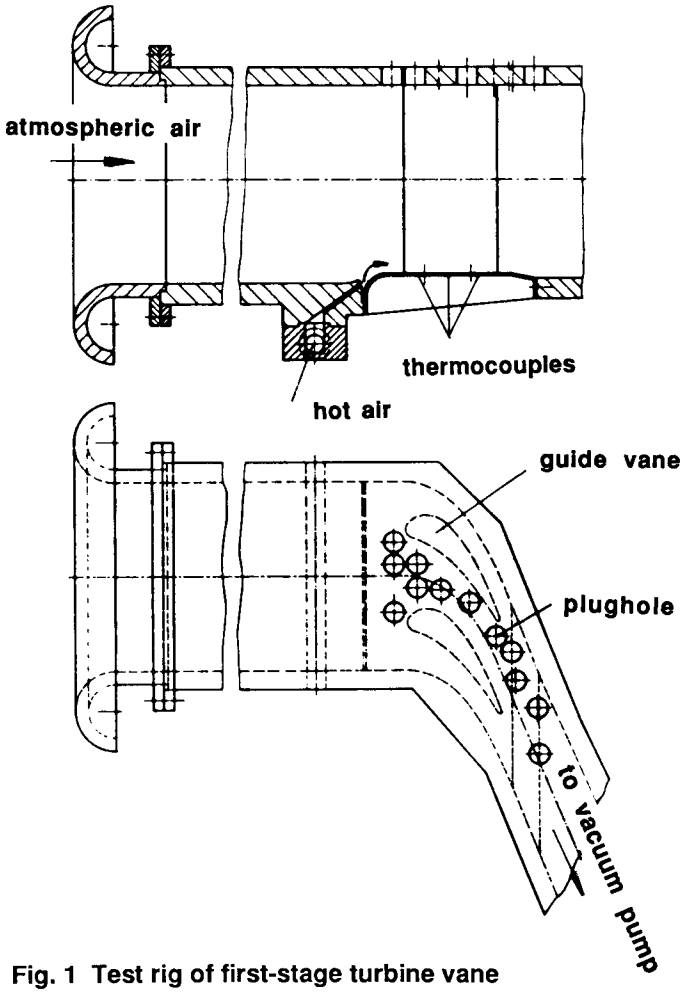

Fig. 1 Test rig of first-stage turbine vane

This generated a representative inlet endwall boundary layer of about 5 mm thickness. Trip wire were installed near the inlet to avoid flow non-uniformities. The lower duct wall contained a slot for film injection. Deviating from gas turbine conditions the cold film was replaced by hot air, which was supplied by a compressor and heated up electrically. A uniform flow distribution inside the slot was achieved using a perforated plate in the supply line.

With respect to the very limited capacity of the vacuum pump, which sucked in the ambient air, the linear vane cascade was reduced to only a single flow passage, lined by two vanes and two passages with only half spacing on each side. The vanes were bonded to the upper duct wall. A rake with thermocouples could be passed through holes in this wall. To maintain a smooth surface and to avoid flow disturbances, the holes not in use were sealed by plugs. The position of these plug holes is also indicated in Fig. 1.

The lower endwall, adjacent to the slot, consisted of a plate of 1.5 mm thickness, made of stainless steel with a thermal conductivity of 15 W/mK. It was instrumented with thermocouples. For the pressure measurements it was replaced by a piece of plexiglass equipped with pressure tappings. All parts of the test rig in contact with hot air were insulated. During the experiment the temperature of the ambient air as well as the hot air flow were measured with thermocouples. The mass-flow of the hot air was measured with a flow meter.

With the thermocouple rake shown in Fig. 2 detailed temperature measurements were carried out within the flow field. Four thermocouples of 0.5 mm diameter were passed through a tube serving as a support. The tube was guided in a plug and could be moved in spanwise direction by a positioning screw. A position transmitter was connected with the tube to measure the distance to the endwall. Temperatures could be measured along a circle with 30 mm diameter by turning the thermocouple rake in the plug.

Before carrying out the temperature measurements the rake was mounted on a special calibration rig to determine the recovery coefficients. Different values between 0.75 and 0.8 were found depending on the angle between flow and thermocouple. During the experiments the recorded data were stored for further processing.

From repeated measurements with the thermocouple rake a scatter of $\pm$ 0.6 K was found. The thermocouples within the endwall include an additional error because of heat conduction in the stainless steel plates which was calculated to be less than 1.4 K. Film temperature and ambient temperature have been measured with an accuracy of 0.2 K.

Fig. 2 Thermocouple rake

Test Program

The mainstream Mach and Reynolds numbers were maintained constant during all tests. The hot gas temperature was kept at about 90 °C. Film mass flow was varied yielding blowing ratios between 0.097 and 2.3, and momentum ratios between 0.01 and 7.3.

To get a visual impression of the flow inside the vane passage, ink was injected onto the endwall near the slot exit. Results are shown in Figs. 3 and 4. They demonstrate an obvious influence of the film on the secondary flow.

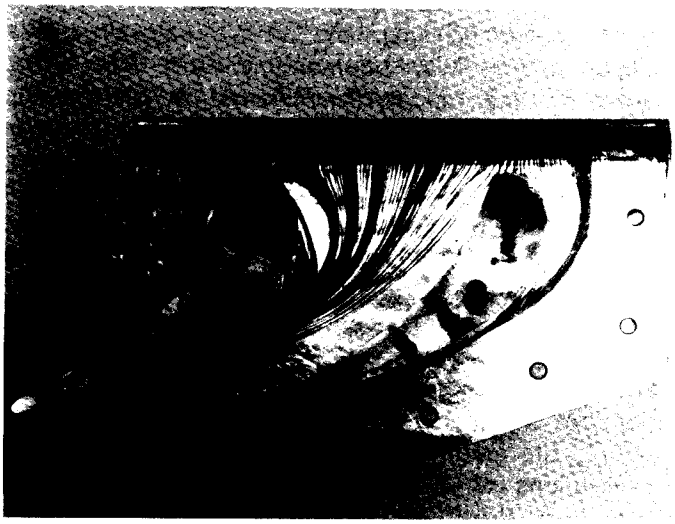

Fig. 3 Visualized surface streamline without film

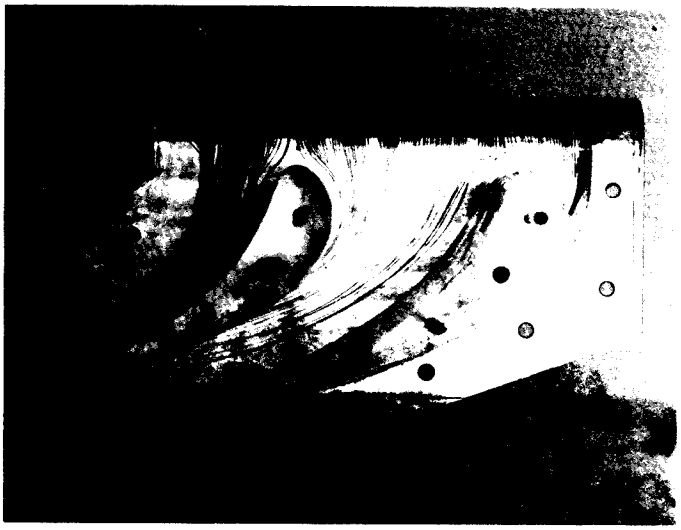

Fig. 4 Visualized surface streamlines, with film (I=0.56)

Fig. 3 shows the situation without any film flow. In some parts of the flow field there are no ink traces at all. This indicates that the endwall boundary layer is moved around the leading edge and across the passage towards the suction side of the vanes. Thus the injected ink is prevented from wetting the endwall near the pressure side of the vane. The limits of the wetted zone are the separation lines where the horseshoe vortex starts to roll up. This separation line turns around the leading edge and reaches the next profile at the suction side at about half-chord position. There the flow is partly leaving the endwall and rising onto the suction surface of the airfoil. Towards the opposite direction, the separation line contacts the airfoil at about quarter-chord position on the suction side.

Fig. 4 shows the flow field on the endwall with a typical cooling film (momentum ratio 0.56). The separation line across the channel is now moved towards mid-channel and reaches the suction side of the next airfoil further downstream. Near the leading edge the separation line is closer to the airfoil. It appears as if the secondary flow has been reduced and surface streamlines have approached the mainstream.

A similar result has been reported by Bourguignon (1985). If we assume that the film reduces the boundary layer thickness, which has to be rebuilt behind the slot, this result also agrees with observations of Jilek (1986). He reported that the secondary flow was more intensive with thick boundary layers than with thin ones.

To measure the adiabatic wall temperatures the test rig was first operated without film flow until a steady state had been reached. The adiabatic wall temperature was measured and the film was switched on and kept constant. During the tests the wall temperatures were measured continuously. From the steady state the film cooling effectiveness was calculated as

$$\eta = \frac{T_W - T_{ad}}{T_F - T_{ad}}$$

with T_w wall temperature with film
T_{ad} adiabatic wall temperature without film
T_F film temperature at slot exit

Some experimental results for three selected blowing rates are shown in Fig. 5.

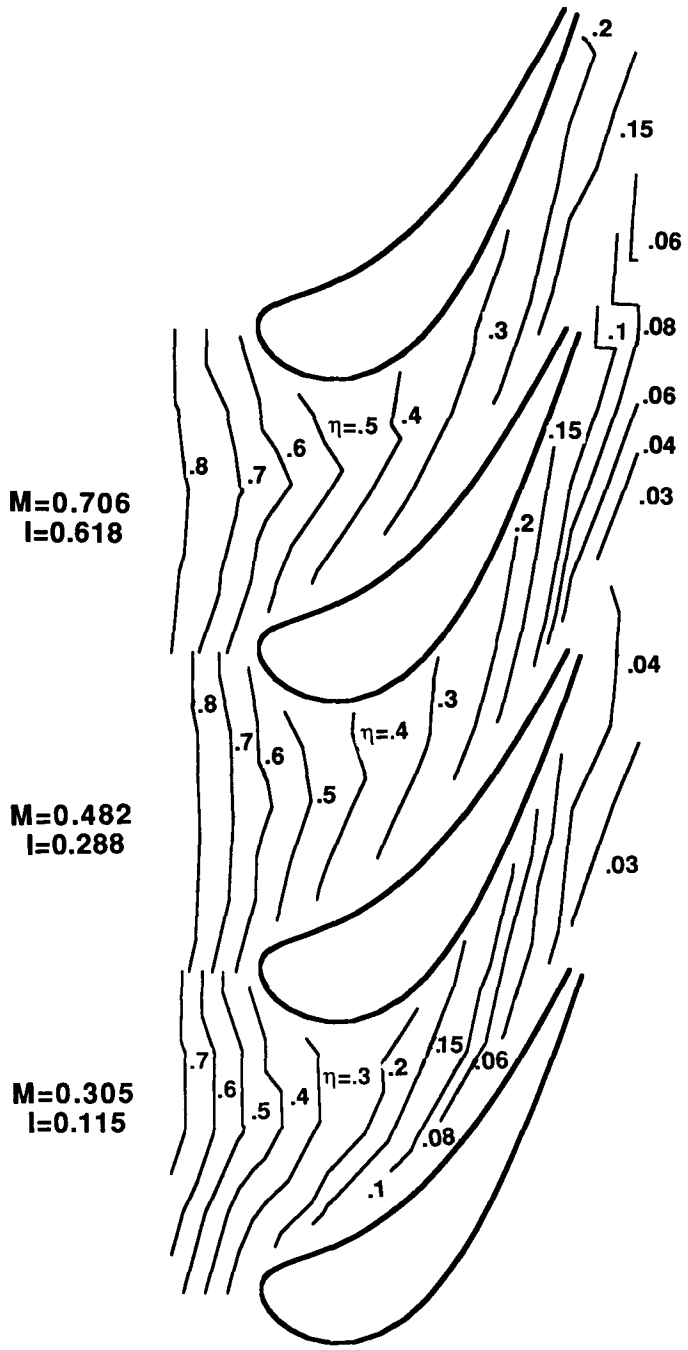

Fig. 5 Film cooling effectiveness, experimental results

Corresponding with the surface streamlines the film cooling effectiveness near the suction side is higher than that near the pressure side. For most parts of the shroud and for low momentum ratios it increases nearly proportionally to the blowing rate.

Numerical Analysis

The basic equations which describe the 3D flow field in the cascade, i.e. the Navier-Stokes equations and the equations for conservation of mass and energy, form an elliptic system. Therefore, in general, a simultaneous solution for the entire flow field is essential. Since detailed discretization is needed to model friction effects near solid surfaces, extensive computer times are required. For thin boundary layers this problem can be simplified by dividing the flow field into an inviscid outer flow, which defines the pressure field, and a boundary layer which can be modelled by solving the parabolic boundary layer equations without altering the pressure distribution. In case of dominant secondary flows, however, the strong vortex system, which is caused by friction, influences the pressure field in the entire cross section of the flow field.

A compromise between solving the fully elliptic equations and conventional boundary layer theory is the partially-parabolic method. It has already been proposed by Patankar and Spalding (1972), and was further developed, e.g. by Moore and Moore (1980). The computer code we applied is based on this approach. It has been written by Lawerenz (1984) and (1986) for gas turbine flows. It involves body fitted coordinates for discretization and, in the version applied here, the Prandtl mixing-length for modelling of turbulence.

The solution is obtained iteratively, starting with the inviscid flow, resulting from the DENTON code (Denton, 1983), and followed by a solution of the parabolized Navier-Stokes equations, where the derivatives in the direction of the mainstream have been neglected in the friction term. With this approach the local mass balance is not strictly conserved. The continuity defect is expressed in terms of a pressure correction, which is added again to the inviscid flow equations. Therefore, by solving the inviscid flow equations and the parabolized Navier-Stokes equations alternatively, the iteration includes the reaction of the friction forces and secondary flow to the pressure field. The iteration is repeated until the pressure correction remains below a given limit.

First test runs by Lawerenz (1986) have demonstrated that the secondary flow field as well as friction losses can be modelled satisfactorily with this approach. The model is restricted to flows where a local back flow within the boundary layer is not important for the entire flow field. Here a separation occurs in the horseshoe vortex in front of the leading edge which causes local back flow. The code overcomes this problem by restricting the wall shear stress to small but positiv values there. This means that the code predicts stagnation instead of local back flow. Therefore the calculated flow field is wrong in the local area in front of the leading edge.

We extended this computer code to include a cooling film, which can be injected tangentially in front of the computational mesh. As turbulence has been modelled here with the mixing-length theory, the influence of cooling film injection on the mixing-length had to be taken into account. For 2D boundary layers such influence has already been modelled by Cary et al. (1979). Applying their model, the mixing-length profiles at the shroud vary continuously from the inlet profiles of slot and mainstream to an equilibrium profile at the stage exit. For 3D boundary layers the distance from the slot, in streamwise direction, is replaced by the contour length of the mainstream.

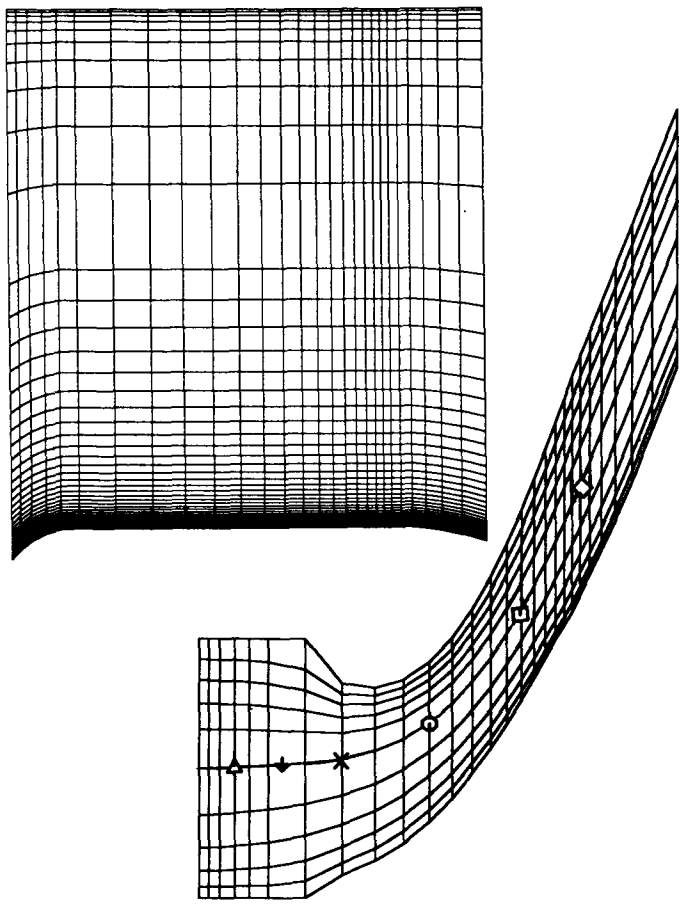

Fig. 6 Computational mesh (symbols refer to Figs. 10 and 11)

The model of Cary et al. (1979) is restricted to tangential slot injection. Moreover, the film must stay attached to the shroud. We expect that this model can approximate our boundary layer sufficiently closely behind the slot. There the turbulent mixing will be enhanced by slot injection, which agrees with our experimental results. The model cannot, however, describe turbulence of typical 3D boundary layer phenomena, e.g. mixing in the horseshoe vortex.

The computational mesh applied here is shown in Fig. 6. It approximates the geometry within the gas turbine, so it differs from the experiment by its strictly periodic boundary conditions from channel to channel. The mesh starts immediately behind the slot, close to the leading edge. A mesh of 25 x 50 x 11 grid points has been used (axial x radial x circumferential) with a minimum wall distance of 0.05% channel height. This is about 1.5% of the boundary layer thickness in front of the slot.

Comparison of Results

A special, typical blowing rate has been selected for comparison of numerical results with the experiments. The physical parameters are listed in Tab. 1. The numerical iteration starts with the 3D pressure field of the inviscid flow. Since the experiment showed no measurable influence of the cooling film to the pressure field, the cooling film has been neglected for this starting solution. Fig. 7 shows, for comparison, the wall pressure at the shroud as measured and as calculated. Significant deviations occur only near the trailing edge. This could also be caused by insufficient periodicity due to the fact that only two blades were installed in the experimental cascade.

The measured film cooling effectiveness is compared with the predicted one in Fig. 8. According to the experiment the film cooling effectiveness decreases from 80% near the slot to 15% at the trailing edge. The variation from blade to blade, however, is greater in the numerical result than in the experiment: The numerical result indicates that

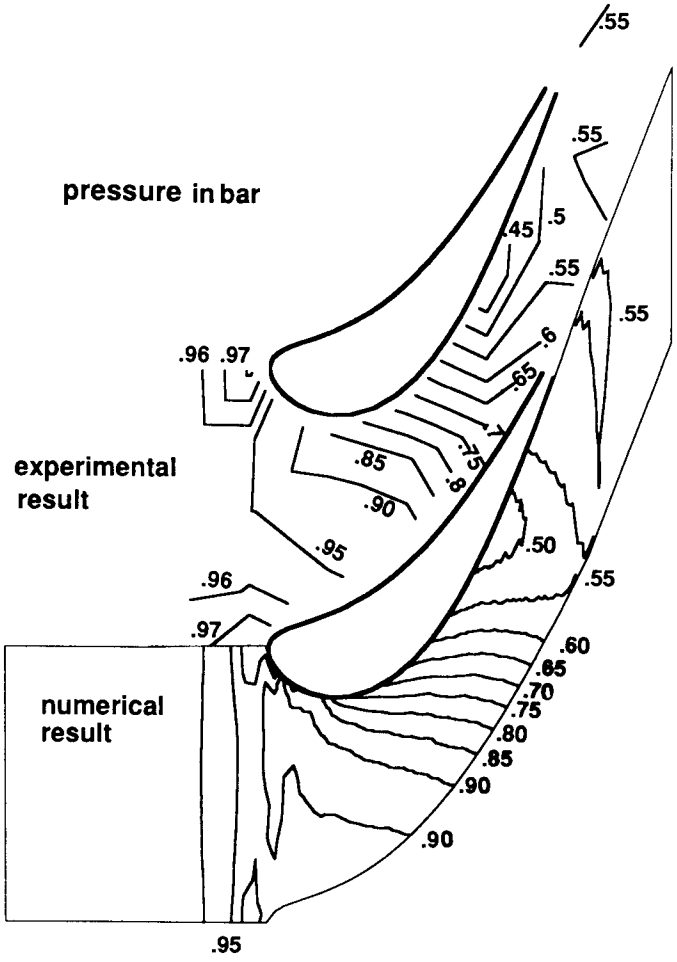

Fig. 7 Static wall pressure at the shroud

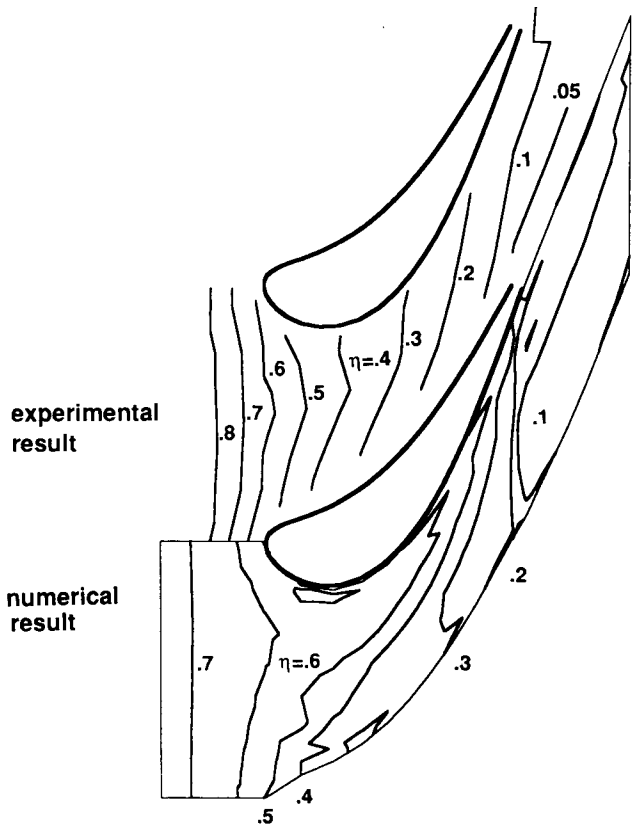

Fig. 8 Film cooling effectiveness at the shroud

the film is concentrated in a vortex which is located on the suction side of the channel. This impression is also confirmed by the cross section temperature distribution and flow pattern, calculated at the trailing edge and shown in Fig. 9. There the temperature has been scaled as

$$\theta = \frac{T_{tot} - T_{inf}}{T_F - T_{inf}}$$

with T_{tot} total temperature,
T_{inf} mainstream temperature,
T_F film temperature at slot exit.

Although this numerical result is very similar to observations by Gaugler and Russel (1983) and Moore and Smith (1984), it differs from the experiment which, in contrast, demonstrates better mixing in circumferential direction.

Temperature measurements in the flow field confirm this difference. For 3 selected points at about mid-channel, we see in Fig. 10 that the temperature profiles also reveal better mixing than predicted. As the horseshoe vortex is badly modelled in the numerical analysis, we conclude that too little turbulent mixing is predicted in this region. Indeed, because of missing back flow regions, the predicted streamlines are smoother than expected. This difference leads to decreased mixing. Moreover, we mentioned above that the extended mixing-length model of Cary et al. (1979) could fail for this application.

We conclude from these results, however, that the applied model is still a good basis for further refinements.

The endwall ink traces cannot be compared with the numerical results, because the laminar sublayer on the endwall has only been approximated by wall functions. Only the turbulent part of the boundary layer has been modelled numerically. Then the calculated velocity at the wall is proportional to the shear stress velocity as described by Lawerenz (1984). In 3D boundary layers this velocity is not parallel to the velocity closest to the wall. This means that surface streamlines are not calculated.

On the suction side of the airfoil the cooling film climbs up to about 6 mm which can be detected at the separation line of the ink traces. This penetration height can be checked against a correlation of Sharma and Butler (1986). We obtain that the predicted penetration height, due to this correlation, is 40% higher than measured. On the other hand, our numerical result agrees perfectly with our measurements.

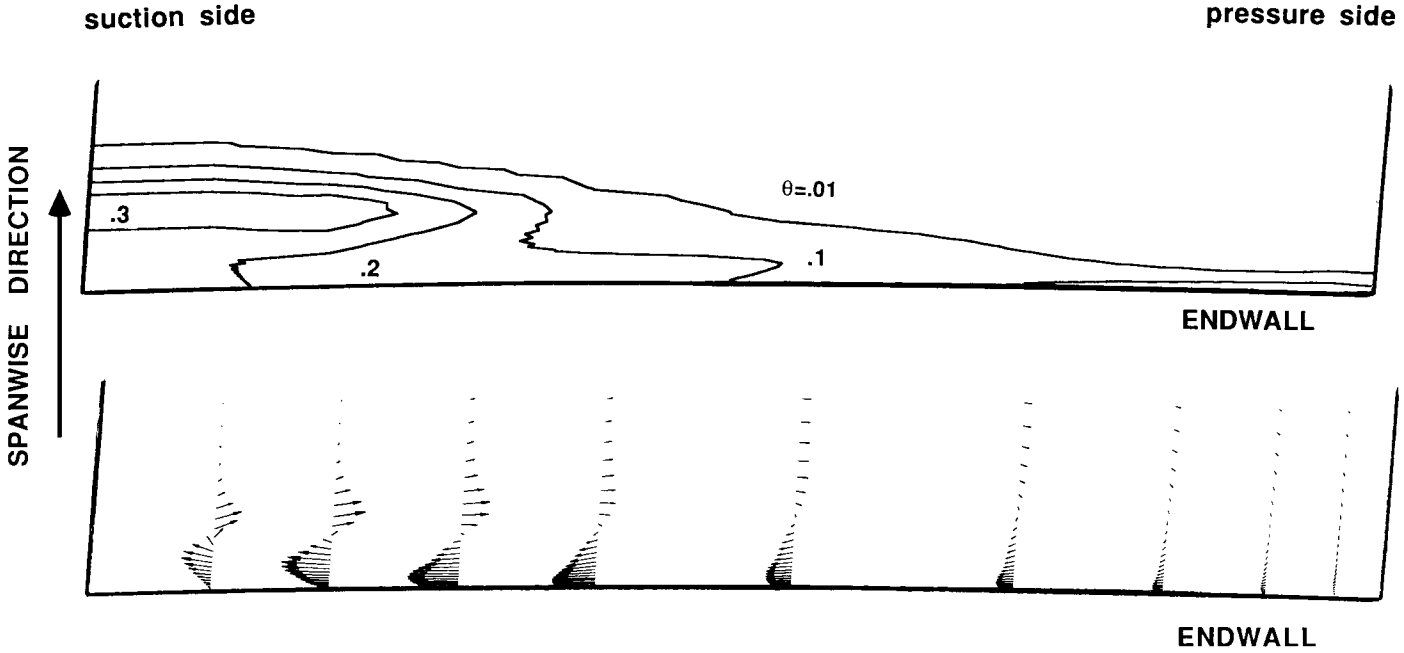

Fig. 9 Dimensionless temperature and secondary flow pattern; cross section at the trailing edge

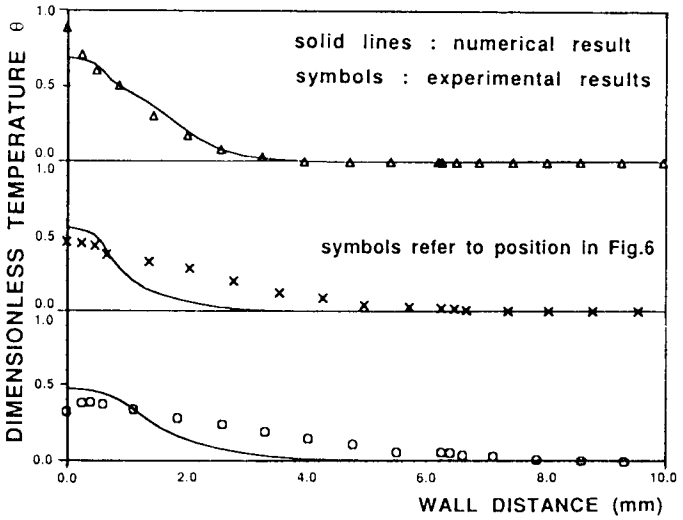

Fig. 10 Dimensionless temperature near mid-channel; comparison of experimental with numerical results

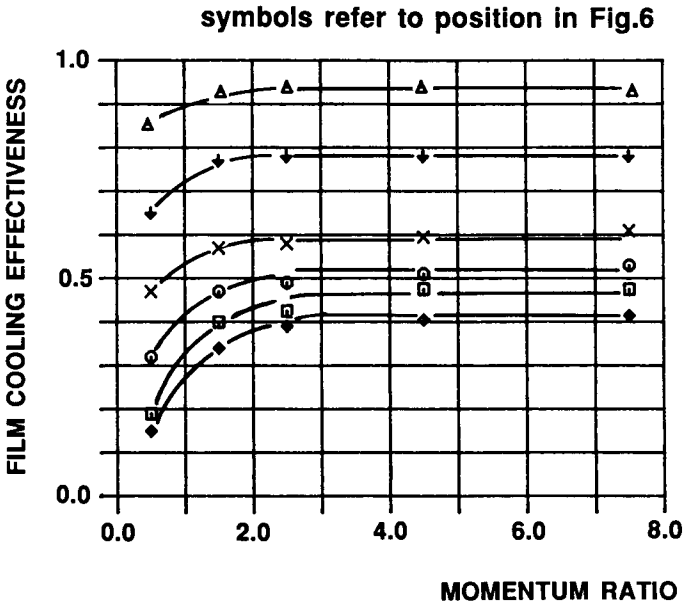

Fig. 11 Film cooling effectiveness at high momentum ratios; experimental results

Application

In order to demonstrate an application, the film cooling effectiveness under real gas turbine conditions will be estimated from the experiments. Geometry and Mach number have been chosen identical to those of the gas turbine. The Reynolds number, based on the mainstream properties, is about half of the gas turbine application because of lower temperatures and pressures. As the cooling film has been replaced by a hot film in the experiment, additional considerations about the scaling of film parameters are required.

As long as the film is added underneath the mainstream and does not penetrate it, the film cooling effectiveness increases monotonically with the blowing rate. The reason is the increasing heat capacity of the coolant. According to data of Pedersen et al. (1977), the film stays attached to the wall in this way if the blowing rate is less than one. Then the density ratio will not effect the film cooling effectiveness, and the experimental results can be applied directly to the gas turbine conditions at equal blowing rates. The model assumptions of the code applied here are also limited to this case.

For blowing rates in excess of one the momentum ratio exceeds 1.25 in our experiments, so that the film penetrates into the mainstream. Accordingly, we can see in Fig. 11 that the film cooling effectiveness does not increase anymore if the momentum ratio exceeds about 2.5. For these high blowing rates, the film cooling effectiveness is a function of both momentum ratio and blowing rate. It was not possible in the experiment to simulate both parameters independently. Therefore, the experimental results are not applicable in this case.

Conclusions

Film cooling effectiveness of a first stage turbine vane shroud has been studied both by experiment and by numerical modelling. It was our aim to develop a numerical tool to predict film cooling effectiveness at the shroud under gas turbine conditions. By comparing the numerical results with the experiment the accuracy of the program was examined.

The model applied here is already encouraging, but further refinements can be suggested. We assume that the k-ε-model will be the more general turbulence model, instead of the mixing-length model applied here. Moreover, a full 3D Navier-Stokes solver could model the endwall boundary layer in more detail than the code applied here. These improvements, however, will also increase the computer time, so that they can only be justified if an increase in accuracy can be achieved.

Tab. 1 Parameters of the test case

blade height	142 mm
chord length	100 mm
spacing	72 mm
slot width	2 mm
thickness of the slot lip	1.8 mm
injection angle	36º
inlet Mach number	0.20
exit Mach number	0.77
exit Reynolds number	720 000
mainstream temperature	20ºC
film temperature	90ºC
blowing rate, M=	0.67
momentum ratio, I=	0.56

References:

Bourguignon, A.E., 1985, "Etudes des Transferts Thermiques sur les Plates-Formes de Distributeur de Turbine avec et sans Film de Refroidissement", AGARD-CP-390

Cary, A.M., Bushnell, D.M., Hefner, J.N., 1979, "Predicted Effects of Tangential Slot Injection on Turbulent Boundary Layer Flow Over a Wide Speed Range", J. Heat Transfer 101, 699-704

Dawes., W.N., 1986, "A Numerical Method for the Analysis of 3D Viscous Compressible Flow in Turbine Cascades; Application to Secondary Flow Development in a Cascade With and Without Dihedral", ASME 86-GT-145

Denton, J.D., 1983, "An Improved Time-Marching Method for Turbomachinery Flow Calculations", J. Eng. of Power 105, 514-524

Gaugler, R.E., Russell, L.M., 1983, "Comparison of Visualized Turbine Endwall Secondary Flows and Measured Heat Transfer Patterns", ASME 83-GT-83

Jilek, J., 1986, "An Experimental Investigation of the Three-Dimensional Flow Within Large Scale Turbine Cascades", ASME 86-GT-170

Langston, L.S., 1980, "Crossflow in a Turbine Cascade Passage", J. Eng. Power 102, 866-874

Lawerenz, M., 1984, "Secondary Flows and Endwall Boundary Layers in Axial Turbomachines", von Karman Institutes, Lecture Series 1984-05

Lawerenz, M., 1986, "Ein Beitrag zur Berechnung der dreidimensionalen reibungsbehafteten Strömung durch axiale Turbinengitter", PhD Thesis University Aachen

Moore, J., Moore, J.G., 1980, "Three-Dimensional, Viscous Flow Calculations for Assessing the Thermodynamic Performance of Centrifugal Compressors - Study of the Eckardt Compressor", AGARD-CP-282

Moore, J., Smith, B.L., 1984, "Flow in a Turbine Cascade: Part 2 - Measurement of Flow Trajectories by Ethylene Detection", J. Eng. Gas Turbines and Power 106, 409-413

Patankar, S.W., Spalding, D.B., 1972, "A Calculation Procedure for Heat, Mass, and Momentum Transfer in Three-Dimensional Parabolic Flows", Int. J. Heat Mass Transfer 15, 1787-1806

Pedersen, D.R., Eckert, E.R.G., Goldstein, R.J., 1977, "Film Cooling With Large Density Differences Between the Mainstream and the Secondary Fluid Measured by the Heat-Mass Transfer Analogy", J. Heat Transfer 99, 620-627

Schulenberg, T., Bals, H., 1987, "Blade Temperature Measurements of Model V84.2 100 MW/60 Hz Gas Turbine", ASME 87-GT-135

Sharma, O.P., Butler, T.L., 1986, "Prediction of Endwall Losses and Secondary Flows in Axial Flow Turbine Cascades", ASME 86-GT-288